J. Fluid Mech. (1991), *vol.* 224, *pp.* 197–215
Printed in Great Britain

The interactive breakdown in supersonic ramp flow

By F. T. SMITH AND A. FARID KHORRAMI
Department of Mathematics, University College London, Gower Street, London WC1E 6BT, UK

(Received 18 October 1989)

The separating flow induced on a ramp under a supersonic main stream is discussed, for high Reynolds numbers, according to the interactive-boundary-layer approach. There are two principal motivations for the study, apart from the recent general upsurge of interest in compressible boundary-layer separation and stall. The first is the need for more progress to be made in the numerical determination of strongly reversed flows than has proved possible in computations hitherto. This is tackled by means of a new computational scheme based in effect on a global Newton iteration procedure but coupled with linearized shooting, second-order accurate windward differencing and linear multi-sweeping. The specific case addressed is the triple-deck version for steady laminar two-dimensional motion, although the present scheme, like the theory described below, also has broader application, for example to subsonic, hypersonic and/or unsteady interactive flows. The second motivation is to compare closely with the recent theoretical prediction (Smith 1988*a*) of a local breakdown or stall occurring in any interactive boundary-layer solution at a finite value of the controlling parameter, α say, within the reversed-flow region; the breakdown produces a large adverse pressure gradient and minimum negative surface shear locally. The first quantitative comparisons are made between the theory and computational results, derived in this work at values of α, here the scaled ramp angle, greater than those obtainable before, but with a fixed outer boundary. The agreement, while not complete, seems to prove fairly affirmative overall and tends to support the suggestion (in Smith 1988*a*) that, contrary to most earlier expectations, in general there is a finite upper limit on the extent to which the interacting boundary-layer approach can be taken on its own. A similar conclusion holds for unsteady interactive boundary layers concerning a finite-time breakdown (Smith 1988*b*) and boundary-layer transition, and in the present context the local nonlinear breakdown provides an explanation for the severe computational difficulties encountered previously as well as for a form of airfoil stall.

1. Introduction

The build-up from small-scale to large-scale separating flow at high Reynolds numbers is of much interest, in aerodynamics, atmospheric dynamics, physiological flows and internal machinery dynamics especially, and two of the most intriguing issues are those of stall and transition. Viscous–inviscid interaction methods have captured many important computational and analytical aspects of such separating flow, in boundary layers, ducts, cascades and so on, as reviewed by Stewartson (1974, 1981), Messiter (1983), Sychev (1987), Smith (1982, 1986*b*), Davis & Werle (1982), for example. The methods and associated composite schemes are most efficient and accurate at medium-to-high Reynolds numbers and have been applied in various

guises to both two- and three-dimensional motions, mostly in the laminar steady regime although there has been some progress also for unsteady flows, concerning transition and dynamic stall, and turbulence-modelled flows. In the aerodynamic context, viscous–inviscid interaction typically links the pressure on the airfoil surface and the boundary-layer displacement, with both being unknown; so in the presence of a sufficiently large disturbance, represented by a non-dimensional parameter α say, flow separation can be encountered in a regular fashion, followed by flow reversal and, depending on the flow configuration, reattachment further downstream. Again see the reviews above.

As a result, there have been many physically interesting and accurate computations of steady interactive separating motions presented in the literature. These are based on various numerical approaches. Examples are the following: the nonlinear shooting techniques of Stewartson & Williams (1969, 1973), Smith & Stewartson (1973), Gajjar (1983), Bodonyi & Smith (1986), Elliott & Smith (1986), Gittler & Kluwick (1987*a*, *b*); the artificial-time marching of Rizzetta, Burggraf & Jenson (1978), Werle *et al.* (1979), Napolitano, Werle & Davis (1978); the inverse and semi-inverse schemes of Carter (1972), Veldman (1981), R. T. Davis (1981 private communication; see also Davis & Werle 1982), Smith (1977), Bodonyi & Smith (1985), Williams (1989); the mixed method of Smith & Merkin (1982), Smith (1985, 1986*a*); the pseudo-spectral approach of Duck & Burggraf (1982), Duck (1985); the alternating-direction methods of Davis (1984); the viscous-dominated approach of Smith (1987, see also later); and several mixtures of these approaches (see also references in the above papers). These include large bodies of work on both the high-Reynolds-number limits, such as the triple-deck version, and the finite-Reynolds-number interpretations through interacting boundary layers, for subsonic, supersonic and hypersonic-limit boundary layers, liquid-layer flows, channel and pipe flows, etc.

The present study is motivated by interest in compressible boundary-layer separation, but also, in particular, by a recent theoretical prediction (Smith 1988*a*) which points to a nonlinear breakdown occurring in the steady interactive-flow solution at a finite value of the disturbance parameter α. The proposed breakdown singularity arises locally within the reversed-flow region and involves a discontinuity appearing in the pressure solution and hence in the reversed velocity profiles: see also (1.2) below. As Smith (1988*a*) observes, this breakdown theory provides an explanation for the severe numerical difficulties which arise in all separated-flow computations (such as those above) once the reversed flow becomes sizeable, as well as for two specific local features that are quite commonly encountered, an accentuated negative minimum in the surface shear stress and an accentuated adverse pressure gradient (see also (1.2)). Comparisons, of a qualitative nature by and large, between the theory and previous interactive computations, Navier–Stokes-based computations, and experiments, are presented by Smith (1988*a*) and seem fairly favourable overall. The theory, moreover, has broad application as it applies to all the interactive-flow separations known to date, with different interpretations for α as described in the above reference. For airfoil flows it has significant repercussions on the build-up from small- to large-scale separations associated with increasing α, since it represents a stall in the sense of a substantial change being induced in the local flow structure. A similar conclusion applies to the somewhat analogous nonlinear break-up at finite time predicted theoretically in Smith (1988*b*) for any unsteady interactive boundary layer, and compared recently with computational studies by J. D. A. Walker & V. Peridier (1989 private communi-

cation; see also Peridier, Walker & Smith 1988, 1990 and Conlisk 1989), the break-up being associated with dynamic stall and boundary-layer transition.

Here a quantitative numerical comparison with the breakdown theory of Smith (1988*a*) is attempted for a specific case of steady separating motion, the supersonic-ramp problem, at increased α values, given the encouraging qualitative comparisons at relatively low α values discussed in the last reference. It appears to be the first such attempt. The current computational work, described below, also seems to enable somewhat more progress to be made in the determination of strongly reversed flow than appears to have been possible in computations hitherto. This is achieved by means of a new computational scheme based in effect on a global Newton iteration procedure, coupled with linearized shooting and with second-order-accurate windward differencing and linear multi-sweeping to accommodate the reversed-flow properties encountered. The new scheme can be applied in principle to other interactive flows including the subsonic and hypersonic regimes, with relatively minor modifications, although here we concentrate specifically on the supersonic case and on the comparison with theory noted above.

The global Reynolds number Re is based on the airfoil chord, say, and the free-stream speed, as are the non-dimensionalized streamwise and normal coordinates x, y and velocity components u, v respectively. In addition, the triple-deck local scalings are then applied near the start of the ramp or concave corner at $x = x_0$, so that for the steady laminar two-dimensional supersonic flow of concern here

$$[x-x_0, y, u, v, p-p_\infty] \rightarrow [Re^{-\frac{3}{8}} b_1 x, Re^{-\frac{5}{8}} b_2 y, Re^{-\frac{1}{8}} b_3 u, Re^{-\frac{3}{8}} b_4 v, Re^{-\frac{1}{4}} b_5 p] \qquad (1.1)$$

in the lower deck, and the ramp angle is $Re^{-\frac{1}{4}} b_6 \alpha$. Here the constants b_n involve powers of the order-one skin-friction factor of the oncoming boundary layer ahead of the ramp, $(M_\infty^2 - 1)$, where $M_\infty > 1$ is the local free-stream Mach number, and the Chapman constant. These scales and the triple-deck arguments lead to the governing interacting-boundary-layer equations given in §2 below; other examples of interacting boundary layers to which the same equations apply with small modifications are given in Smith (1988*a*). The theory of Smith (1988*a*) is also summarized in §2, its major predictions being that, within the reversed-flow region for some finite $\alpha = \alpha_s$,

$$\max\left(\frac{dp}{dx}\right) \rightarrow +\infty, \quad \min\,(\tau_w) \rightarrow -\infty, \qquad (1.2a, b)$$

with

$$\frac{\max(dp/dx)}{[\min(\tau_w)]^2} \rightarrow O(1) \quad \text{as} \quad \alpha \rightarrow \alpha_s^-, \qquad (1.2c)$$

where τ_w is the scaled skin friction. The computational procedure is described in §3. The main results and comparisons are then presented in §4, and again, partly for definiteness and partly to compare closely with the theory, the outer boundary in the normal direction is kept fixed in most of the computations described, since in particular the theory applies for any value of the outer-boundary edge used. The comparisons with the predictions in (1.2), while not entirely conclusive, tend to be fairly affirmative overall, and hence to confirm the view that contrary to many earlier expectations there is a finite upper limit on how far the interacting-boundary-layer approach can be taken on its own. Further discussion is also presented in §4.

2. The governing equations, and the proposed breakdown structure

The triple-deck version of the interactive boundary-layer formulation appropriate to high Reynolds numbers is tackled here, although other versions including the interpretation(s) at finite Reynolds numbers are equally susceptible in principle to the theoretical breakdown as noted by Smith (1988*a*). We decided to concentrate on the problem of supersonic flow over a ramp partly for its own practical interest and partly because it represents a characteristic viscous–inviscid interactive flow which has received considerable attention previously, in particular from Rizzetta *et al.* (1978) and (as kindly pointed out to us by a referee) from Ruban (1978), and which can produce separated flow at sufficiently large ramp angles. Thus the governing equations in normalized form are the two-dimensional steady boundary-layer equations,

$$u = \frac{\partial \psi}{\partial y}, \quad v = -\frac{\partial \psi}{\partial x}, \tag{2.1a}$$

$$u\frac{\partial u}{\partial x} + v\frac{\partial u}{\partial y} = -p'(x) + \frac{\partial^2 u}{\partial y^2}, \tag{2.1b}$$

holding in the lower deck, subject to the constraints

$$u = v = 0 \quad \text{at} \quad y = 0, \tag{2.1c}$$

$$u \sim y + A(x) + \alpha f(x) \quad \text{as} \quad y \to \infty, \tag{2.1d}$$

$$\left[u, v, p, \frac{\mathrm{d}A}{\mathrm{d}x}\right] \to \begin{cases} [y, 0, 0, 0] & \text{as} \quad x \to -\infty, \quad (2.1e) \\ [y, 0, \alpha, -\alpha] & \text{as} \quad x \to +\infty, \quad (2.1f) \end{cases}$$

$$p(x) = -\frac{\mathrm{d}A}{\mathrm{d}x}, \tag{2.1g}$$

respectively for no slip at the solid surface, matching with the main-deck flow solution, merging with the parallel flows far upstream and far downstream, and pressure-displacement interaction. This last is Ackeret's result derived from the supersonic potential flow properties applying in the upper deck outside the boundary layer. A Prandtl shift has been applied above, so that the surface shape is represented by $\alpha f(x)$ where, for the ramp case,

$$f(x) = 0 \quad (\text{for } x < 0), \quad f(x) = x \quad (\text{for } x > 0). \tag{2.1h}$$

The parameter α, here taken to be positive, gauges the relative angle of the ramp or concave corner. The closed problem (2.1*a–h*) is elliptic because of an eigen or branching solution that starts at large negative x, representing upstream influence.

Interest centres then on the properties of (2.1) as α increases and in particular the advent of separated or reversed flow. Numerous computational treatments of (2.1) and related flow problems have been given previously including the approaches based on nonlinear shooting, artificial time-marching, inverse and semi-inverse schemes, alternating direction-implicit and -explicit, mixed inverse sweeping, (pseudo-)spectral, and others, as described for example in §1. All the methods so far appear to meet with about the same degree of success, namely accurate solutions are computed with a limited amount of reversed flow present but numerical accuracy

and convergence are lost as the reversed flow strengthens. Further, a pronounced negative minimum is observable in the skin friction $\tau_w \equiv \tau(x,0)$ (where $\tau \equiv \partial u/\partial y$) locally within the reversed-flow zone, in some of the computations, along with a significant adverse pressure gradient.

These two features of the computed results, the numerical difficulties and the solution behaviour in reversed flow, led to the recent theoretical suggestion (Smith 1988*a*) of a singularity or breakdown arising in the interactive-boundary-layer solution at a finite value of α. The proposed breakdown, say as $\alpha \to \alpha_s^-$, is a predominantly inviscid process taking place within a short streamwise lengthscale $O(\hat{A})$ surrounding the reversed-flow breakdown position $x = x_s$, where u, ψ, p are typically $O(1)$. Thus the controlling equations reduce to the inviscid form

$$u = \frac{\partial \psi}{\partial y}, \quad V = -\frac{\partial \psi}{\partial X}, \tag{2.2a}$$

$$u\frac{\partial u}{\partial X} + V\frac{\partial u}{\partial y} = -\frac{\mathrm{d}p}{\mathrm{d}X}, \tag{2.2b}$$

from (2.1*a*, *b*), with $x - x_s = \hat{A}X$, subject to the displacement condition at large y and the tangential-flow condition near the surface,

$$u \sim y + \beta_0 \quad \text{as} \quad y \to \infty, \tag{2.2c}$$

$$\psi = 0 \quad \text{at} \quad y = 0+. \tag{2.2d}$$

Here $\beta_0 \equiv A(x_s) + \alpha_s f(x_s)$ is a finite constant, and (2.2*d*) is consistent with the existence of a viscous sublayer of thickness $O(\hat{A}^{\frac{3}{2}})$ adjoining the surface and containing reversed motion. The reversed velocity profiles at the streamwise ends of this thin breakdown region are different,

$$u \to u_1(y) \quad \text{upstream}, \quad u \to u_2(y) \quad \text{downstream}, \quad \text{with } u_1 \not\equiv u_2, \tag{2.2e}$$

and cause an overall pressure rise, so that

$$p(x_s^-) < p(x_s^+) \quad \text{at} \quad \alpha = \alpha_s. \tag{2.3}$$

Again, it follows that the maximum pressure gradient induced is large, $O(\hat{A}^{-1})$, and positive, and the minimum in the skin friction is large, $O(\hat{A}^{-\frac{1}{2}})$, but negative:

$$\max\left(\frac{\mathrm{d}p}{\mathrm{d}x}\right) \sim \hat{A}^{-1}, \quad \min(\tau_w) \sim -\hat{A}^{-\frac{1}{2}}, \tag{2.4a, b}$$

with $\hat{A} \to 0+$ as $\alpha \to \alpha_s^-$. The proposed relation between $\hat{A}$ and $(\alpha_s - \alpha)$ stems from the relative effects of the viscous sublayer thickness and the displacement $(-A)$ variation induced by the Ackeret law (2.1*g*), in this case, suggesting the scale

$$\hat{A} = (\alpha_s - \alpha)^2. \tag{2.4c}$$

Virtually the same reasoning behind(2.2)–(2.4*b*) applies to all the viscous–inviscid interactive flows known to date (with only (2.4*c*) being altered): see Smith (1988*a*), which also proposes other forms of finite-α breakdown, although the above is the main form. Further, a not dissimilar breakdown phenomenon is described by Smith (1988*b*) for unsteady interactive boundary layers, the singularity in that context

arising at a finite time. Here we concentrate on the steady supersonic-ramp problem (2.1) and describe a computational approach designed to go further into the separated-flow regime at higher α values than has proved possible before, in order to extend the capability of reversed-flow computations as well as to compare more closely with the theoretical predictions in (2.2)–(2.4) of a finite-α breakdown.

3. The numerical approach

The scheme developed is basically a global Newton procedure but coupled with linearized marching and a second-order-accurate treatment of any reversed flow encountered. The classical Newton approach of assuming

$$[\psi, u, \tau, p, A] = [\bar{\psi}, \bar{u}, \bar{\tau}, \bar{p}, \bar{A}] + [\tilde{\psi}, \tilde{u}, \tilde{\tau}, \tilde{p}, \tilde{A}] \tag{3.1}$$

is taken, in an ψ–u–τ formulation, with the differences (tilde variables) between the unknown solution on the left and the given guess (overbar variables) being supposed to be small. Hence $(\tilde{\psi}, \tilde{u}, \tilde{\tau})(x, y)$, $\tilde{p}(x)$, $\tilde{A}(x)$ are governed by the linearized system

$$\tilde{u} - \frac{\partial \tilde{\psi}}{\partial y} = \frac{\partial \bar{\psi}}{\partial y} - \bar{u}, \quad \tilde{\tau} - \frac{\partial \tilde{u}}{\partial y} = \frac{\partial \bar{u}}{\partial y} - \bar{\tau}, \tag{3.2a}$$

$$\left(\bar{u}\frac{\partial \tilde{u}}{\partial x} + \tilde{u}\frac{\partial \bar{u}}{\partial x} - \frac{\partial \bar{\psi}}{\partial x}\tilde{\tau} - \frac{\partial \tilde{\psi}}{\partial x}\bar{\tau}\right) + \frac{\mathrm{d}\tilde{p}}{\mathrm{d}x} - \frac{\partial \tilde{\tau}}{\partial y} = -\left(\bar{u}\frac{\partial \bar{u}}{\partial x} - \frac{\partial \bar{\psi}}{\partial x}\bar{\tau} + \frac{\mathrm{d}\bar{p}}{\mathrm{d}x} - \frac{\partial \bar{\tau}}{\partial y}\right), \tag{3.2b}$$

subject to the boundary conditions.

$$\tilde{u} = -\bar{u}, \quad \tilde{\psi} = -\bar{\psi} \quad \text{at} \quad y = 0, \tag{3.2c}$$

$$\tilde{u} - \tilde{A}(x) \sim (y + \bar{A}(x) + \alpha f(x) - \bar{u}) \quad \text{as} \quad y \to \infty, \tag{3.2d}$$

$$\left[\tilde{\psi}, \tilde{u}, \tilde{\tau}, \tilde{p}, \frac{\mathrm{d}\tilde{A}}{\mathrm{d}\tilde{x}}\right] \to \begin{cases} \{\frac{1}{2}y^2 - \bar{\psi},\ y - \bar{u},\ 1 - \bar{\tau},\ -\bar{p},\ -\mathrm{d}\bar{A}/\mathrm{d}x\] & (x \to -\infty), \quad (3.2e) \\ [\frac{1}{2}y^2 - \bar{\psi},\ y - \bar{u},\ 1 - \bar{\tau},\ \alpha - \bar{p},\ -\alpha - \mathrm{d}\bar{A}/\mathrm{d}x] & (x \to \infty), \quad (3.2f) \end{cases}$$

$$\tilde{p} + \frac{\mathrm{d}\tilde{A}}{\mathrm{d}x} = -\left(\bar{p} + \frac{\mathrm{d}\bar{A}}{\mathrm{d}x}\right), \tag{3.2g}$$

from (2.1a–g). The broad object then is to reduce all the right-hand sides in (3.2a–g) as closely to zero as possible, by repeatedly solving for the tilde variables and adding them to the overbarred variables to obtain new global guesses as implied in (3.1).

The method used is as follows; see also figure 1. Finite differencing of second-order accuracy is applied to (3.2), with step sizes Δx, Δy in x, y, to yield the discretized system

$$\tfrac{1}{2}(\tilde{u}_{ij+1} + \tilde{u}_{ij}) - (\tilde{\psi}_{ij+1} - \tilde{\psi}_{ij})/\Delta y = (\bar{\psi}_{ij+1} - \bar{\psi}_{ij})/\Delta y - \tfrac{1}{2}(\bar{u}_{ij+1} + \bar{u}_{ij}), \tag{3.3a}$$

$$\tfrac{1}{2}(\tilde{\tau}_{ij+1} + \tilde{\tau}_{ij}) - (\tilde{u}_{ij+1} - \tilde{u}_{ij})/\Delta y = (\bar{u}_{ij+1} - \bar{u}_{ij})/\Delta y - \tfrac{1}{2}(\tilde{\tau}_{ij+1} + \tilde{\tau}_{ij}), \tag{3.3b}$$

$$\begin{aligned} &[\bar{\bar{u}}(\tilde{u}_{ij+1} + \tilde{u}_{ij} - \tilde{u}_{i-1j+1} - \tilde{u}_{i-1j})/2\Delta x + \tfrac{1}{4}(\tilde{u}_{ij+1} + \tilde{u}_{ij} + \tilde{u}_{i-1j+1} + \tilde{u}_{i-1j})\,\bar{\bar{u}}' \\ &\quad - \tfrac{1}{4}(\tilde{\tau}_{ij+1} + \tilde{\tau}_{ij} + \tilde{\tau}_{i-1j+1} + \tilde{\tau}_{i-1j})\,\bar{\bar{\psi}}' - \bar{\bar{\tau}}(\tilde{\psi}_{ij+1} + \tilde{\psi}_{ij} - \tilde{\psi}_{i-1j+1} - \tilde{\psi}_{i-1j})/2\Delta x] \\ &\quad + (\tilde{p}_i - \tilde{p}_{i-1})/\Delta x - (\tilde{\tau}_{ij+1} - \tilde{\tau}_{ij} + \tilde{\tau}_{i-1j+1} - \tilde{\tau}_{i-1j})/2\Delta y \\ &= -[\bar{\bar{u}}\bar{\bar{u}}' - \bar{\bar{\psi}}'\bar{\bar{\tau}} + (\bar{p}_i - \bar{p}_{i-1})/\Delta x - (\bar{\tau}_{ij+1} - \bar{\tau}_{ij} + \bar{\tau}_{i-1j+1} - \bar{\tau}_{i-1j})/2\Delta y], \end{aligned} \tag{3.3c}$$

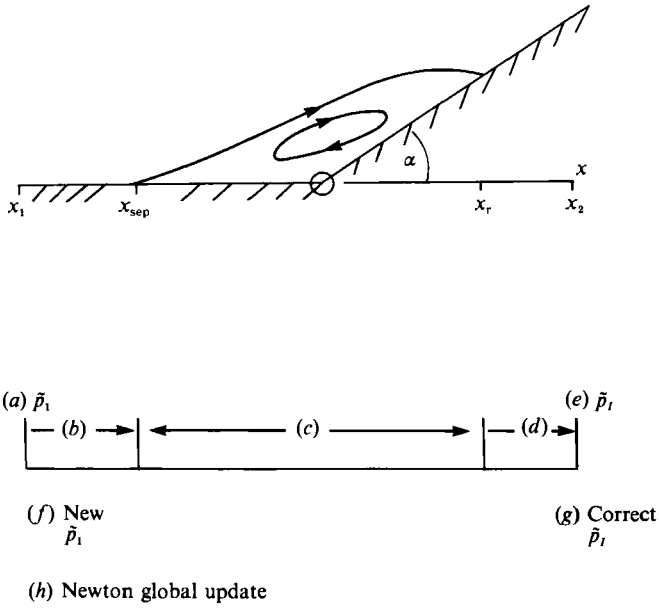

FIGURE 1. Diagram indicating the global iteration scheme based on linearized shooting: (*a*) guess $\tilde{p}_1$; (*b*) march forward; (*c*) sweep back and forth; (*d*) march forward to downstream end; (*e*) store $\tilde{p}_I$; (*f*) reguess $\tilde{p}_1$ and repeat (*b*)–(*e*); (*g*) interpolate to obtain correct end condition on $\tilde{p}_I$; (*h*) update global solution, and restart at (*a*).

where

$$\bar{\bar{u}} \equiv \tfrac{1}{2}(\bar{u}_{ij+1}+\bar{u}_{ij}+\bar{u}_{i-1j+1}+\bar{u}_{i-1j}),$$

$$\bar{\bar{u}}' \equiv (\bar{u}_{ij+1}+\bar{u}_{ij}-\bar{u}_{i-1j+1}-\bar{u}_{i-1j})/2\Delta x,$$

$$\bar{\bar{\psi}}' \equiv (\bar{\psi}_{ij+1}+\bar{\psi}_{ij}-\bar{\psi}_{i-1j+1}-\bar{\psi}_{i-1j})/2\Delta x,$$

$$\bar{\bar{\tau}} \equiv \tfrac{1}{4}(\bar{\tau}_{ij+1}+\bar{\tau}_{ij}+\bar{\tau}_{i-1j+1}+\bar{\tau}_{i-1j}).$$

These are subject to the discretized versions of (3.2*c–g*),

$$\tilde{u}_{i1} = -\bar{u}_{i1}, \quad \tilde{\psi}_{i1} = -\bar{\psi}_{i1}, \tag{3.3d}$$

$$\tilde{u}_{iJ} = (y_J+\bar{A}_i+\alpha f_i-\bar{u}_{iJ})+\tilde{A}_i, \tag{3.3e}$$

the analogue of (3.2*e*, *f*), including $\tilde{p}_I = \alpha-\bar{p}_I$, (3.3*f*)

$$\tfrac{1}{2}(\tilde{p}_i+\tilde{p}_{i-1})+\left(\frac{\tilde{A}_i-\tilde{A}_{i-1}}{\Delta x}\right) = -\tfrac{1}{2}(\bar{p}_i+\bar{p}_{i-1})-\left(\frac{\bar{A}_i-\bar{A}_{i-1}}{\Delta x}\right). \tag{3.3g}$$

Here the streamwise spacing has $x = x_1+(i-1)\,\Delta x$ with i running from 1 (at the upstream end $x = x_1$) to I (at the downstream extreme $x = x_2 = x_1+(I-1)\,\Delta x$); the normal spacing is $y = (j-1)\,\Delta y \equiv y_j$ for $j = 1$ to J; and the subscripts i, j refer to evaluation at the i, j grid point as usual. The condition (3.3*f*) is described more precisely below, and the ends $x = x_1$, x_2, $y = y_J$ are intended to represent the asymptotic extremes shown in (3.2*d–f*). The overbarred and double-overbarred quantities are prescribed for each sweep of the flow field, $1 \leqslant i \leqslant I$, $1 \leqslant j \leqslant J$. The linear boundary-value problem in terms of x is then treated in the following way, if

the flow is totally forward: see the case of reversed flow later. A guess is made for $\tilde{p}_1$, the small pressure kick at the starting station $x = x_1$. The system (3.3*a–e, g*) is then marched forward in x from $i = 2$ to the end station $i = I$ where $x = x_2$ to give an end pressure value $\tilde{p} = \tilde{p}_I$. A second guess for $\tilde{p}_1$, followed by a forward march, yields a second value for $\tilde{p}_I$. Since we require $\tilde{p}_I$ to satisfy the condition (3.3*f*), linear interpolation of the two $\tilde{p}_1$ guesses can be used in principle to obtain the correct value of $\tilde{p}_1$ to achieve this condition. This particular aspect relies of course on the linearity of the system (3.3) being addressed here, yielding an explicit global update solution in effect, as opposed to nonlinear shooting of (2.1) which is implicit and can even encounter nonlinear singularities corresponding to enhanced separation or attached flow during each sweep of the flow field. In the current method, with the correct $\tilde{p}_1$ value found, the solution ($\tilde{\psi}$, $\tilde{u}$, $\tilde{\tau}$, $\tilde{p}$, $\tilde{A}$) is known therefore throughout the flow domain and is added to ($\bar{\psi}$, $\bar{u}$, $\bar{\tau}$, $\bar{p}$, $\bar{A}$) to provide an updated global guess. The procedure, of solving (3.3) by shooting and then updating via (3.1), is continued until a suitable convergence criterion is met.

In more detail, at each i-station (3.3*a–e, g*) can be solved explicitly by matrix inversion, given all the overbarred quantities and the values at the $i-1$ station. At the starting station $i = 1$ we set $\tilde{p}_1$ as described above along with $\tilde{A}_1 = 0$ and $\tilde{\psi} = \tilde{u} = \tilde{\tau} = 0$ at each j-point, and likewise at the end station $i = I$. We ensured that the overbarred variables satisfied all the boundary conditions at the outset, to help matters. Also, a smoothing factor (q) was used for the ramp shape as described later. Again, a relaxation factor ω was added to the updating step corresponding to (3.1), at the higher values of α. Finally here, the downstream growth of the shooting solutions triggered by the guesses for $\tilde{p}_1$ is sufficiently strong that in practice, i.e. on the computers used here, linear interpolation alone is inadequate to achieve the downstream constraint accurately, especially at the higher values of α, during the early sweeps of the flow domain. This growth of linear disturbances is equivalent to the Lighthill (1953) exponential branching behaviour

$$\tilde{p} \propto \exp(\kappa x) \quad (\kappa = 0.8272\ldots) \tag{3.4}$$

persisting as $x \to +\infty$ rather than being confined to its proper role as an upstream-influence factor for $x \to -\infty$ as mentioned in §2. To counteract this, the linear shooting procedure is continued to a maximum of M shoots, with each newly interpolated $\tilde{p}_1$ value serving as a new first guess for the correct pressure kick. The counter-action is however switched off well before halfway through the computations, for a given α, as the direct interpolation proves adequate after that stage.

If reversed flow is present, the above scheme is modified for each linear shoot (see figure 1). Given the guessed value of $\tilde{p}_1$, the forward march is taken up to the separation station $x = x_{\text{sep}}$ beyond which some velocity profiles with negative $\bar{u}$ exist. The scheme is then swept repeatedly back (decreasing i) and forth (increasing i) through the reversed-flow region between the separation and the reattachment point $x = x_r$ until the reversed-flow solution is sufficiently converged, say after N sweeps. In this region windward differencing is applied, to stabilize the back and forward marching, in the form

$$\begin{aligned}
&[\bar{\bar{u}}(-3\tilde{u}_{ij+\frac{1}{2}} + 4\tilde{u}_{i+1j+\frac{1}{2}} - \tilde{u}_{i+2j+\frac{1}{2}})/2\Delta x \\
&\quad + \tilde{u}_{ij+\frac{1}{2}}\bar{\bar{u}}' - \bar{\bar{\psi}}'\tilde{\tau}_{ij+\frac{1}{2}} - \bar{\bar{\tau}}(3\tilde{\psi}_{ij+\frac{1}{2}} - 4\tilde{\psi}_{i-1j+\frac{1}{2}} + \tilde{\psi}_{i-2j+\frac{1}{2}})/2\Delta x] \\
&\quad + (3\tilde{p}_i - 4\tilde{p}_{i-1} + \tilde{p}_{i-2})/2\Delta x - (\tilde{\tau}_{ij+1} - \tilde{\tau}_{ij})/\Delta y \\
&= -[\bar{\bar{u}}\bar{\bar{u}}' - \bar{\bar{\psi}}'\bar{\bar{\tau}} + \bar{\bar{p}}' - \bar{\bar{\tau}}^{(1)}],
\end{aligned} \tag{3.5}$$

where $\bar{\bar{u}} = \bar{u}_{ij+\frac{1}{2}}$, $\bar{\bar{u}}' = (-3\bar{u}_{ij+\frac{1}{2}} + 4\bar{u}_{i+1j+\frac{1}{2}} - \bar{u}_{i+2j+\frac{1}{2}})/2\Delta x$,

$\bar{\bar{\psi}}' = (3\bar{\psi}_{ij+\frac{1}{2}} - 4\bar{\psi}_{i-1j+\frac{1}{2}} + \bar{\psi}_{i-2j+\frac{1}{2}})/2\Delta x$, $\bar{\bar{\tau}} = \bar{\tau}_{ij+\frac{1}{2}}$,

$\bar{\bar{p}}' = (3\bar{p}_i - 4\bar{p}_{i-1} + \bar{p}_{i-2})/2\Delta x$, $\bar{\bar{\tau}}^{(1)} = (\bar{\tau}_{ij+1} - \bar{\tau}_{ij})/\Delta y$,

and the subscript $j+\frac{1}{2}$ stands for the average of j and $j+1$ values. Here, for a forward or a back sweep, (3.5) replaces (3.3*c*) at grid points i,j where there is reversed flow, defined by $\bar{u}$ negative, the centring here being at $i,j+\frac{1}{2}$ rather than at $i-\frac{1}{2},j+\frac{1}{2}$ as before and allowing direct upstream propagation of information via the extended streamwise differencing as in $\bar{\bar{u}}'$ above. The form (3.5) for reversed flow preserves the nominal second-order accuracy of the whole approach, and it proved stable. First-order-accurate forms were also tested and these gave, upon grid extrapolation from several runs, results that virtually coincided with those from the above form. (Another stabilizing feature of the linearized method here is that the background field $\bar{u},\bar{v}$, which provides the latest estimates of $x_{\text{sep}}, x_{\text{r}}$ among other things, is 'frozen', and so tends to suppress the growing oscillatory behaviour that often ruins nonlinear iterative computations of separating flows as the reversed motion strengthens.) Once the solution in the reversed-flow domain is settled as above, the remaining interval between x_{r} and the end station x_2 can be covered by marching forward, thus yielding $\tilde{p}_I$, and then the next linear shoot, with another $\tilde{p}_1$ value, is performed in the same manner, in readiness for the linear-interpolation procedure described in the previous paragraph.

The typical grids used in the computations had the parameters (I, Δx, J, Δy, x_1, x_2) equal to (101–201, 0.4–0.2, 41, 0.25, −12, 18) and tests on their effects are illustrated in the figures below. Again, we usually took (q, ω, M, N) equal to (20, 0.1, 15, 20–24) but also tested their influences on the solution and on the speed of convergence. The convergence criterion was set as a difference of 10^{-4} or less between the successive overbarred values of the skin friction and pressure, and this required up to 140 overall flow-field sweeps, i.e. applications of the update corresponding to (3.1), at the higher values of a α tackled and for a typical grid. Computed solutions at such α values were derived by gradual increases from converged results at lower α values. The solutions from the present method also agree closely with those obtained from an alternative linearization method described by Smith (1987) (see also Bowles 1990) in which, in essence, the nonlinear terms on the left-hand side in (2.1*b*) are assumed known, the resultant linearized system (2.1*a–h*) is solved in an elliptic manner for u, v, p, A everywhere, the nonlinear terms are then updated, with much under-relaxation, and the iteration process then continues. This latter method likewise produced accurate solutions up to α values greater than those obtained in previous studies but significantly less than in the current method described in (3.1)–(3.5). The results from the current approach, especially for the much higher α values that proved attainable with apparent accuracy, are presented in the next section.

4. Results, comparisons and discussion

Sample computational results obtained for the skin friction τ_{w} and the pressure p, versus x, are plotted in figures 2 and 3 for various values of α. See also subsequent figures. Grid-size effects and the pressure-gradient maxima are also indicated here and below. Regular separation, flow reversal and reattachment are present for α greater than a value $\alpha_{\text{sep}} \approx 1.57$. Beyond that value the current solutions are in quite close agreement with Rizzetta *et al.*'s (1978) up to α values of about 3 but differ

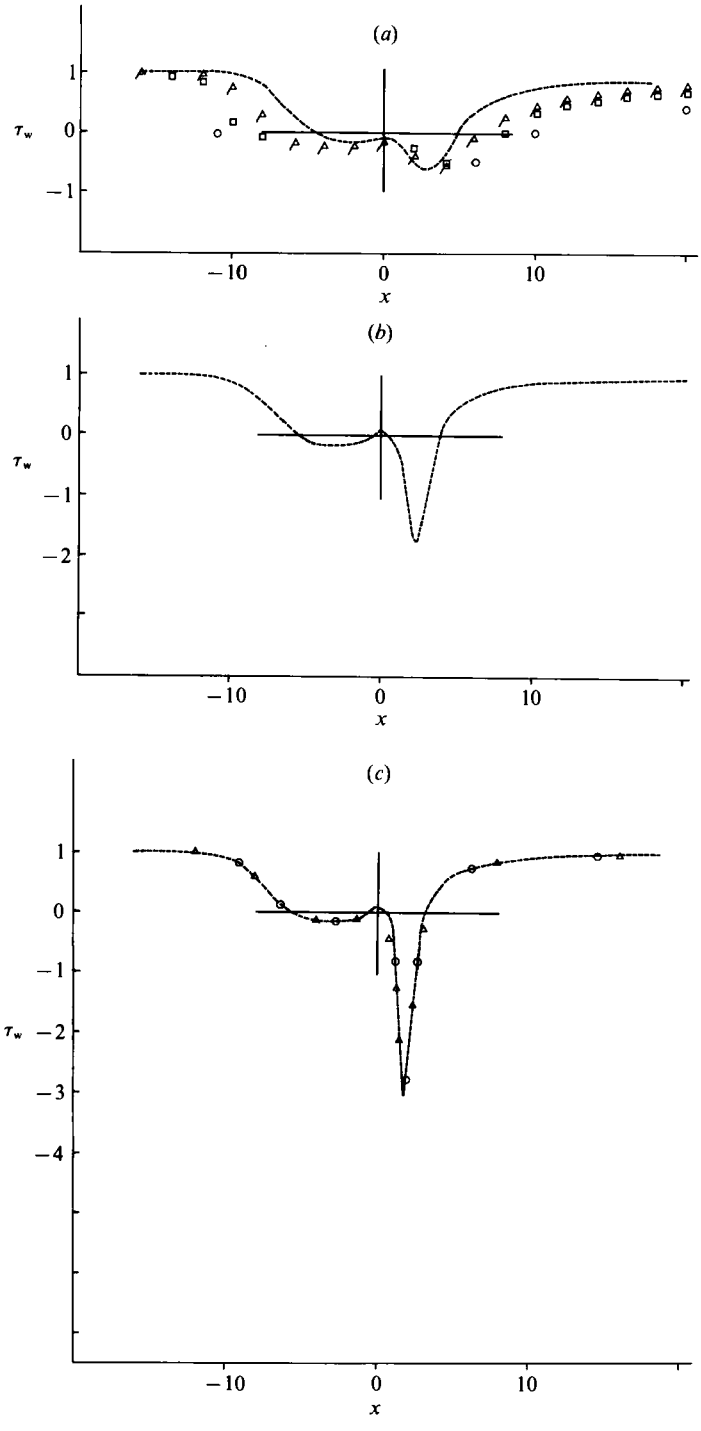

FIGURE 2(a–c). For caption see facing page

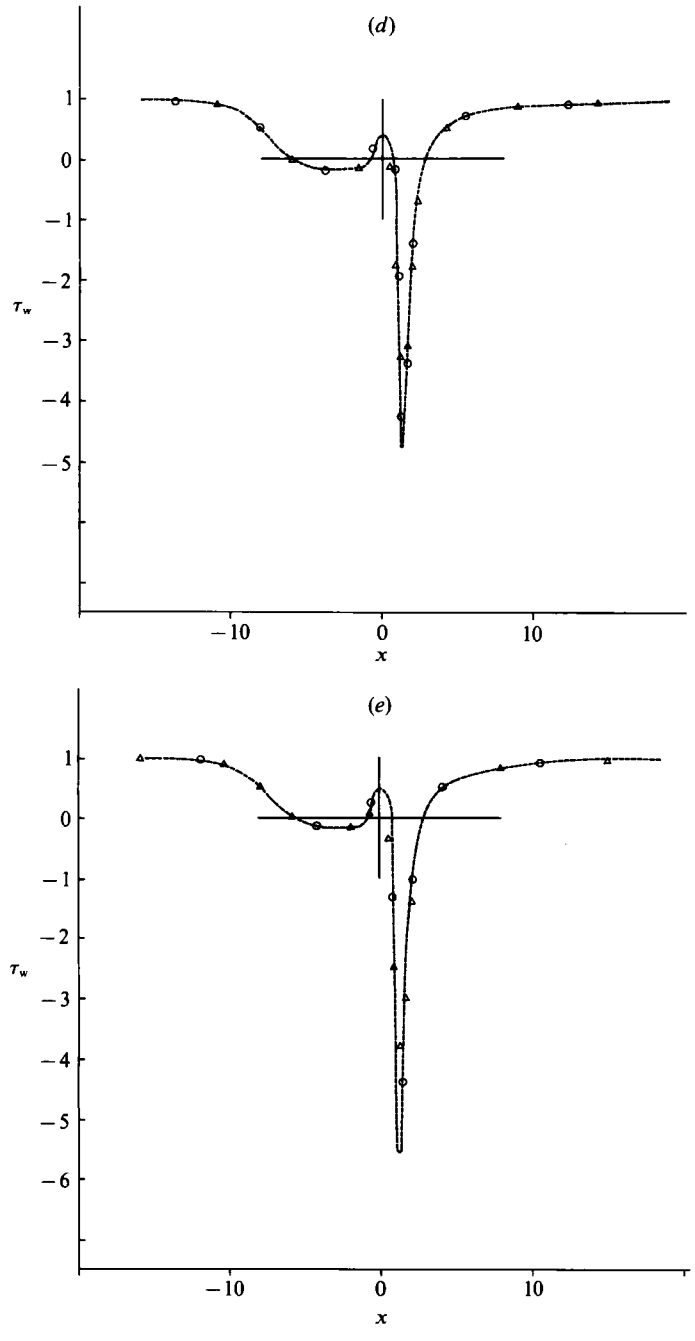

FIGURE 2. Computed solutions for skin friction τ_w versus x for ramp angles (*a*) $\alpha = 3.5$, (*b*) 4.5, (*c*) 5.2, (*d*) 6.2, (*e*) 6.6. Grids used have $[x_1, x_2, \Delta x, y_J, \Delta y, q] = [-16, 24, 0.4, 10, \frac{1}{3}, 20]$ (shown △ in *c–e*), $[-16, 24, 0.2, 10, \frac{1}{3}, 20]$ (shown ---), $[-12, 18, 0.2, 10, \frac{1}{3}, 20]$ (shown ○○○ in *c–e*). Also shown, for $\alpha = 3.5$ in (*a*), are results for $y_J = 15$(△), $y_J = 20$ (□) and Rizzetta *et al*'s results (○). Other grid effects are given in later figures.

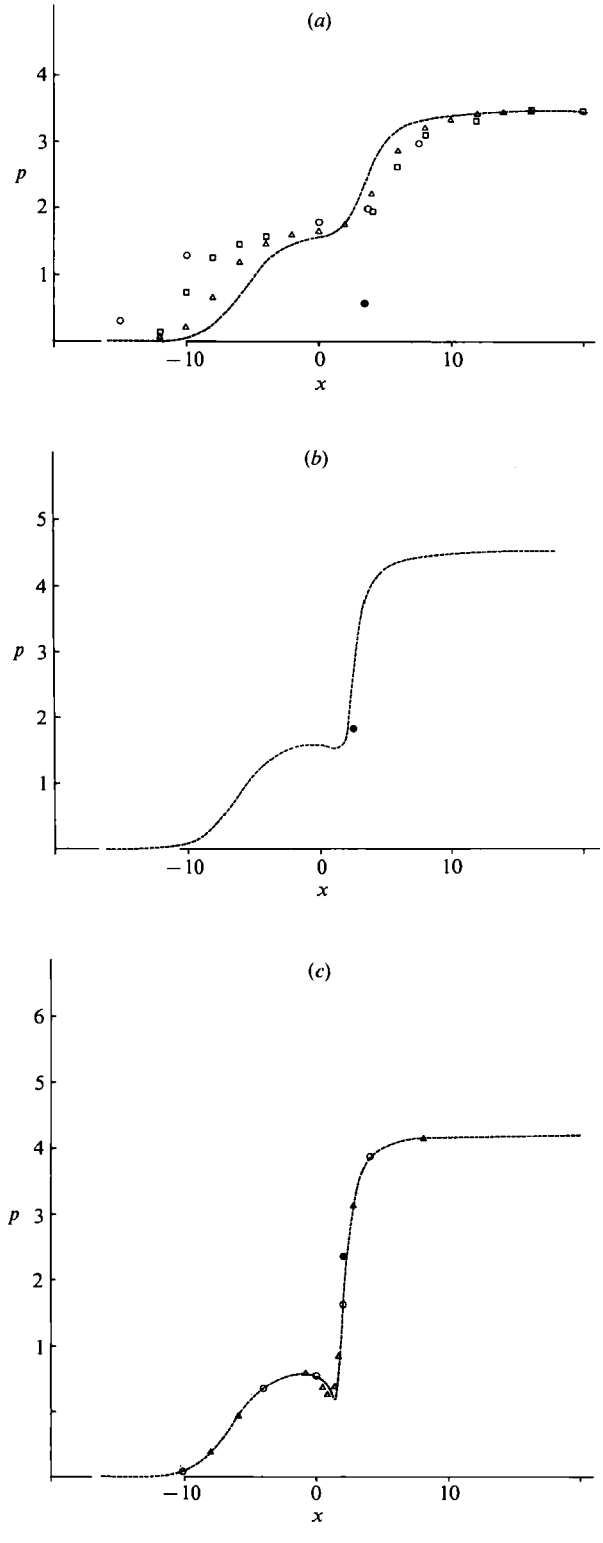

FIGURE 3(a–c). For caption see facing page

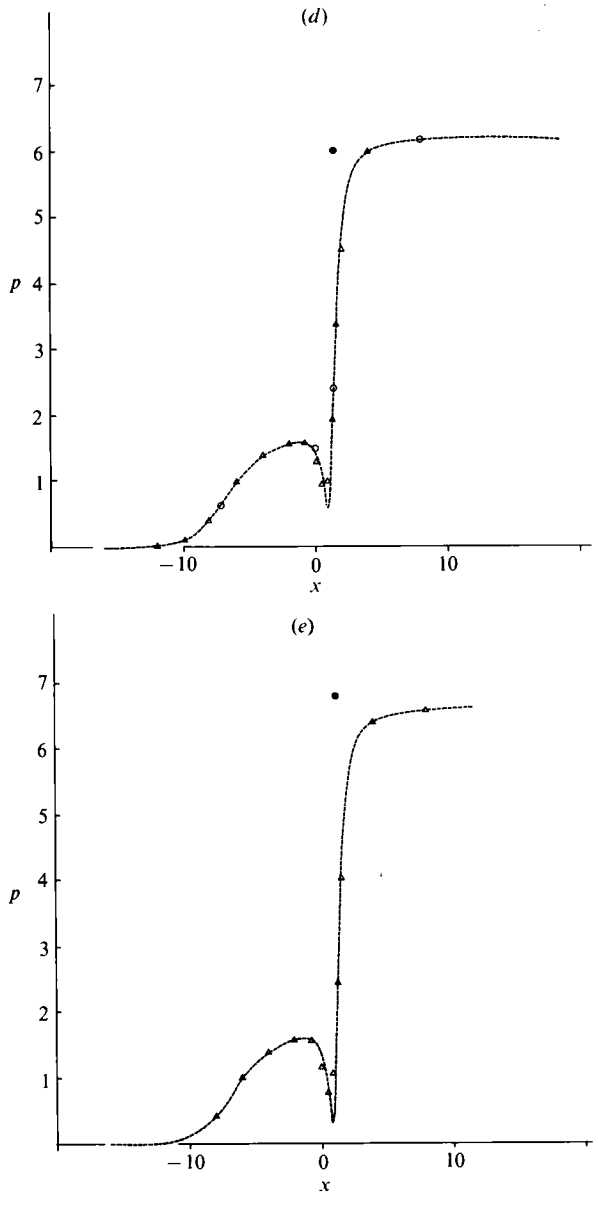

FIGURE 3. Results for the pressure p versus x; same notation as in figure 2. The solid dots denote the values, and locations, of $\max(\mathrm{d}p/\mathrm{d}x)$.

noticeably at the largest value ($\alpha = 3.5$) for which they showed results: Professor O. R. Burggraf (private communication 1988), we note, agrees with the trends of the new results there. Typical velocity profiles are shown in figure 4. The most striking features of the computed solutions at the higher values of α in all the figures 2–4 are: first, the local drop in pressure associated with secondary separation near the corner; second, the halting of the trend towards an increasingly large separation eddy encountered at lower α values (see also below however); and third, the increasingly rapid streamwise variations locally in the reversed-flow domain, with pronounced negative dips being encountered in the skin-friction curves and sharp rises in the

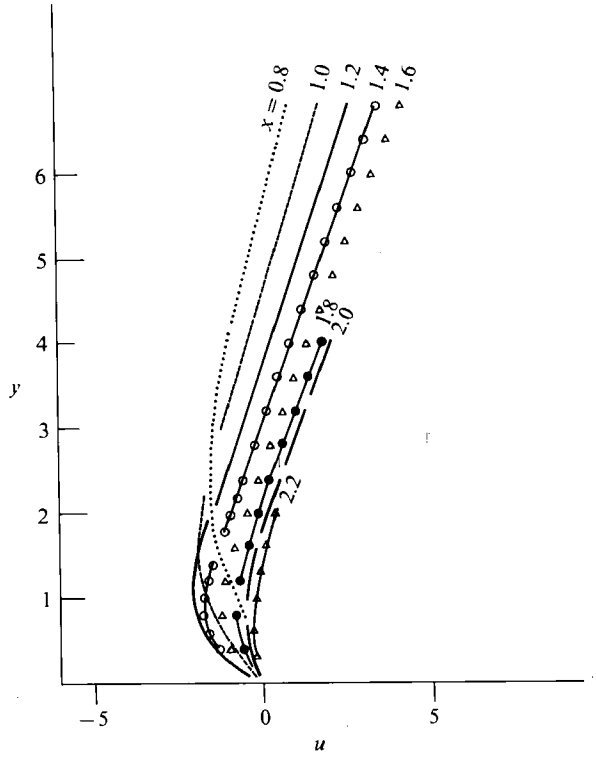

FIGURE 4. Computed velocity profiles for $\alpha = 6.2$, from grid $[-16, 24, 0.2, 10, \frac{1}{3}, 20]$, at various x-stations.

pressure curves, prior to reattachment. It seems fairly clear that these last features are qualitatively in keeping (or not out of keeping) with the theory of Smith (1988*a*) described earlier, as is the character of the velocity profiles.

To make comparisons in quantitative terms, then, at such higher α values, we first present the overall extrema of the computed τ_w, dp/dx solutions within the reversed-flow region, versus α, in figures 5 and 6. These lead on to the plots in figure 7 of the quantities $-1/\min(\tau_w)$ and $[1/\max(dp/dx)]^{\frac{1}{2}}$ versus α, to compare with the particular theoretical predictions in (2.4). The computational results appear to be in reasonably close agreement with the theoretical trend for a relatively wide range of the higher α values. They indicate a critical value α_s somewhat below 9 in this case, subject to the comments below.

Grid-size effects shown in the figures above include results from both the first- and the second-order-accurate windward differencing procedures described in §3, from varying grid spacing in both directions and the outer boundaries, and from altering the ramp shape very close to the corner at $x = 0$. Here the ramp shape (see (2.1*h*)) was replaced by $f(x) = x/\{1 + \exp(-qx)\}$ with q being a relatively large positive constant. Computed solutions were obtained for various values of the smoothing factor q and these appeared to confirm the occurrence of secondary separation near the start of the ramp, as shown in figure 2, as well as indicating no significant effects on the results elsewhere in the flow field. Comparisons are also given with numerical solutions from the alternative linearization approach outlined near the end of §3, the agreement being good. The main effect of the grid distribution is that due to the outer-y boundary throughout, which influences the separation length mentioned

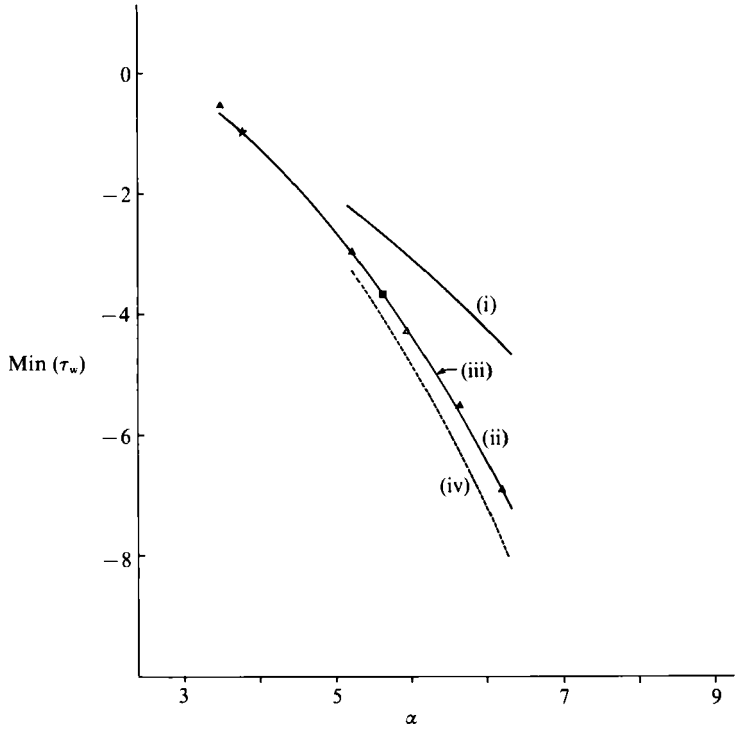

FIGURE 5. Variation of min (τ_w) with α. Results (i) (ii), (iii) correspond to the first three grids listed in the caption for figure 2, in turn, and (iv) is from extrapolation of (i), (ii). Also presented are the results from altering q to 10 (□), y_J to 15 (△ and ▲) in case (ii), and from the alternative linearization method outlined at the end of §3 (shown ★, with $x = 240 \times 0.5$).

earlier for instance, but we decided mainly to focus specifically on the results with the outer-y boundary at 10, for the reasons given in §1, especially considering that the theory above, with which comparisons are made, applies also to finite outer boundaries. (In passing, and in reply to a referee, we note that the decay far downstream is of exponential form for a fixed outer boundary, rather than the algebraic form (e.g. Gittler & Kluwick 1989) holding for infinite outer boundaries.) The computations clearly become considerably more sensitive as regards accuracy as α is increased, even though it proved possible (as indicated partially in the figures) to extend the results to larger α values with a given coarser grid or with only first-order windward differencing. The accuracy limitations along with the corresponding reductions in the overall convergence rates rendered the method increasingly time-consuming at the increased α values covered in this work, but it is felt that the combination of the required links and comparisons with the theory above and the significantly higher α-range accommodated tended to justify the computer time and effort involved.

Both the comparisons with the theory and the extension to more strongly separated flow associated with higher values of α would seem to be fairly encouraging aspects overall. Such comparisons between computations and theory can never be utterly convincing of course. We note among other things that the values shown as extrema in figures 5–7 are the minima or maxima of the values actually obtained at grid points, without interpolation, and so these tend to underestimate the true extrema; similar underestimation of the extrema, and hence overestimation of the

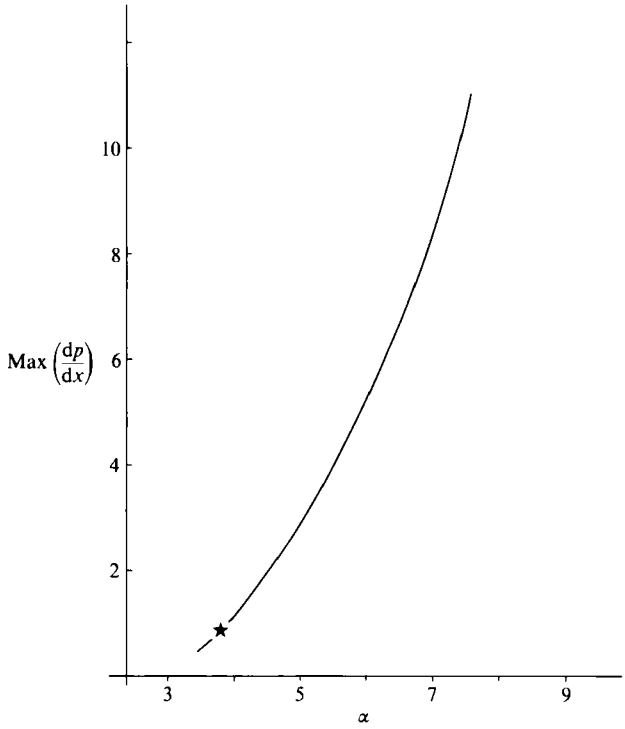

FIGURE 6. Variation of max $(\mathrm{d}p/\mathrm{d}x)$ with α, from the third grid listed in the caption for figure 2. Also shown (★) is the result from the alternative method, as in figure 5.

critical value α_s, is evident in all the grid refinement procedures and extrapolation. Again, the quantities involved, the surface shear and the pressure gradient, are always among the most sensitive quantities to determine numerically. Indeed it could still be the case that, especially for infinite outer boundaries, the interactive-boundary-layer solution may continue to infinitely large α (Smith 1988*a*), given also the possibility of non-uniqueness among other things. Discontinuities or similar phenomena, however, would then seem necessary to overcome the theoretical difficulties described in previous theoretical attempts at providing a large-α solution of the nonlinear system. As far as the numerical study here is concerned, the new method developed appears to have worked fairly well, at least in this context, and to have gone further into the reversed-flow regime than all previous ones, at least as far as we are aware. Other numerical attempts would be very welcome, needless to say, on this and other strongly separated interactive motions, in view of the sensitivity of the computations and the non-uniqueness question for instance.

The theoretical breakdown in Smith (1988*a*) which partly motivated the present investigations is predominantly an inviscid phenomenon (see also §2) and so it leads to an Euler stage next, locally around the breakdown position. This stage, i.e. where the two-dimensional nonlinear Euler equations apply, bringing in non-zero normal pressure gradients as the major extra feature, requires new numerical studies to sort out its impact on the overall motion for example. Work along those lines is being started by one of us (F.T.S.). Physically, the breakdown, which can occur in any interacting boundary layer, is believed to represent the onset of stall in the separating motion corresponding to significant alteration in the flow structure locally. In principle this breakdown can arise in any large-scale breakaway separation

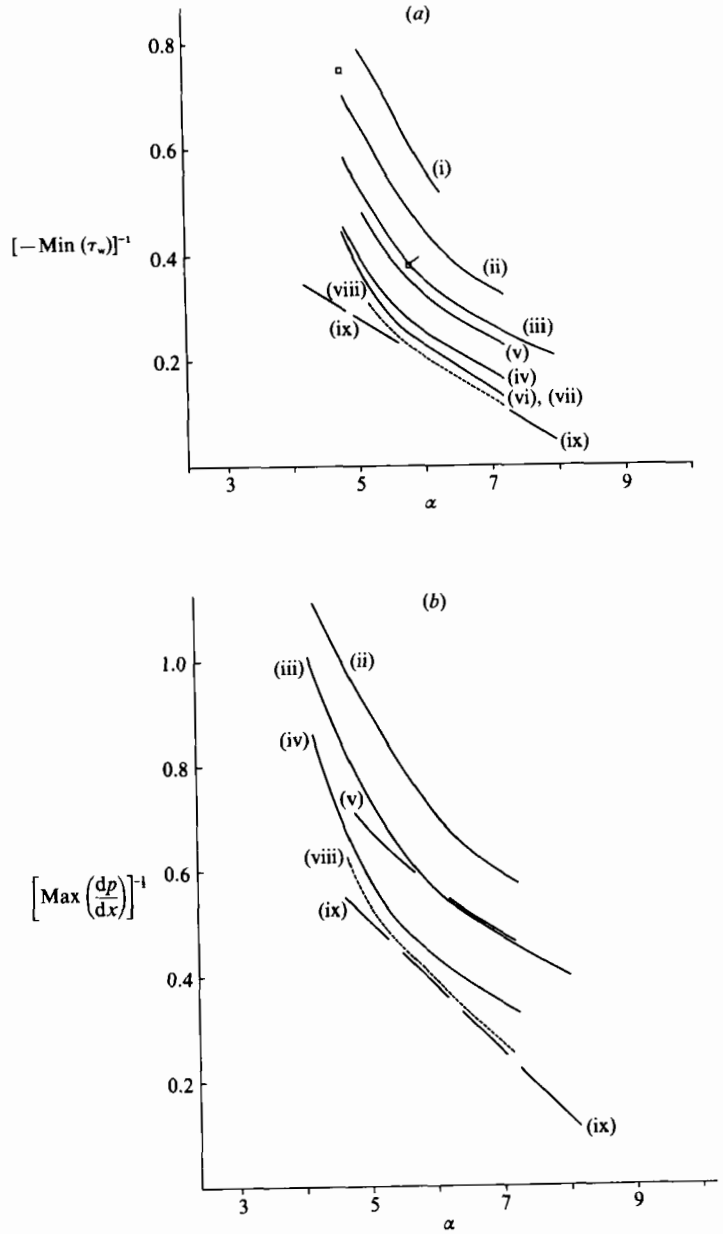

FIGURE 7. Results for (*a*) $[-\min(\tau_w)]^{-1}$ and (*b*) $[\max(dp/dx)]^{-\frac{1}{3}}$, versus α. In (*a*), curves (i), (ii), (iii) are from the first-order-accurate scheme described towards the end of §3, with $\Delta x = 0.8, 0.4, 0.2$ in turn; (iv) is extrapolated from (ii), (iii); curves (v), (vi), (vii) are from the first three successive grids listed in the caption for figure 2 (results (vi), (vii) are graphically identical); curve (viii) is extrapolated from (v), (vi). The same notation applies for (*b*). Also shown is the effect of setting the y-distribution as $y = 50 \times 0.2$ (□′) for case (iii), and $y = 40 \times 0.375$ (□) for case (ii). Curves (ix), in (*a*), (*b*), are straight lines predicted from the theory in (2.4) (Smith 1988*a*), for comparison.

as well as in the more confined regimes such as the supersonic-ramp separation considered here. The occurrence and prediction of stall are of much importance in practical applications, especially for aerodynamics, and the theoretical breakdown form above suggests criteria for the occurrence in steady separating flow: see integral properties of the local velocity profiles in the reference above. Unsteady stall and the allied phenomenon of transition are also of great practical interest and these are addressed in related theoretical work (Smith 1988*b*), yielding a broadly similar local breakdown at finite time. Computational comparisons in the unsteady case, and subsequent theory on the removal of the finite-time-breakdown, are in Peridier, Walker & Smith (1990; see also Peridier 1989), and Hoyle, Smith & Walker (1990; see also Hoyle 1991) respectively. Also, certain unsteady-flow interactions are being tackled with the present computational method (§3), which can also be modified to the subsonic range for instance and has been applied to the interactive hypersonic range by Khorrami & Smith (paper in preparation; see also Brown *et al.* 1991; Khorrami 1991), for steady flows past flat plates and thin airfoils.

Thanks are due to the referees, for helpful comments, to SERC and MOD for joint support of A.F.K., to AFOSR for support for F.T.S., and to SERC and ULCC for Cray computer facilities.

REFERENCES

Bodonyi, R. J. & Smith, F. T. 1985 On short-scale inviscid instabilities in the flow past surface-mounted obstacles and other nonparallel motions. *Aeron. J.* June/July, 205–212.

Bodonyi, R. J. & Smith, F. T. 1986 Shock-wave laminar boundary layer interaction in supercritical transonic flow. *Computers Fluids* **14**, 97–108.

Bowles, R. I. 1990 Applications of nonlinear viscous-inviscid interactions in liquid layer flows and transonic boundary layer transition. Ph.D. thesis, University of London.

Brown, S. N., Khorrami, A. F., Neish, A. & Smith, F. T. 1991 Hypersonic boundary-layer interactions and transition. *Phil. Trans. R. Soc. Lond.* (to appear).

Carter, J. E. 1972 *NASA Tech. Rep.* TR-R-385.

Conlisk, A. T. The pressure field in intense vortex–boundary layer interaction. Presented at Reno, Nevada, January 1989. *AIAA Paper* 89–0293.

Davis, R. T. 1984 *AIAA Paper* 84-1614 (presented at Snowmass, Colorado, June 1984).

Davis, R. T. & Werle, M. J. 1982 Progress on interacting boundary layer computations at high Reynolds numbers. In *Proc. 1st Symp. Num. Phys. Aspects Aerodyn. Flows, Long Beach, CA* (ed. T. Cebeci), pp. 187–210. Springer.

Duck, P. W. 1985 Laminar flow over unsteady humps: the formation of waves. *J. Fluid Mech.* **160**, 465–498.

Duck, P. W. & Burggraf, O. R. 1982 Spectral computation of triple-deck flows. In *Proc. 1st Symp. Num. Phys. Aspects Aerodyn. Flows, Long Beach, CA* (ed. T. Cebeci), pp. 145–158. Springer.

Elliott, J. W. & Smith, F. T. 1986 Separated supersonic flow past a trailing edge at incidence. *Computers Fluids* **14**, 109–116.

Gajjar, J. 1983 On some viscous interaction problems in incompressible fluid flows. Ph.D. thesis, University of London.

Gittler, P. H. & Kluwick, A. 1987*a* Nonuniqueness of triple-deck solutions for axisymmetric supersonic flow with separation. In *Boundary-Layer Separation* (ed. S. N. Brown & F. T. Smith). Springer.

Gittler, P. H. & Kluwick, A. 1987*b* Triple-deck solutions for supersonic flow past flared cylinders. *J. Fluid Mech.* **179**, 469–487.

Gittler, P. H. & Kluwick, A. 1989 Interacting laminar boundary layers in quasi-two-dimensional flow. *Fluid Dyn. Res.* **5**, 29–47.

HOYLE, J. M. 1991 Ph.D. thesis, University of London (in preparation).

HOYLE, J. M., SMITH, F. T. & WALKER, J. D. A. 1990 On sublayer eruption and vortex formation. *Proc. IMACS Conf., Boulder, CO., June 1990* (to appear, 1990, *Computer Phys Commun.*).

KHORRAMI, A. F. 1991 Hypersonic aerodynamics on flat plates and thin airfoils. D.Phil. thesis, University of Oxford (submitted).

LIGHTHILL, M. J. 1953 On boundary layers and upstream influence II. Supersonic flows without separation. *Proc. R. Soc. Lond.* A **217**, 478–507.

MESSITER, A. F. 1983 Boundary-layer interaction theory. *Trans. ASME* E: *J. Appl. Mech.* 50. 1104–1113.

NAPOLITANO, M., WERLE, M. J. & DAVIS, R. T. 1978 Numerical solutions of the triple-deck equations for supersonic and subsonic flow past a hump. *Rep.* AFL-78-6-42. University of Cincinnati; see also *AIAA J.* **17** no. 7, 1979.

PERIDIER, V. J., (1989) Ph.D. thesis, Lehigh University

PERIDIER, V. J., WALKER, J. D. A. & SMITH, F. T. 1988 Methods for the calculation of unsteady separation. *AIAA Paper* 88-0604, presented at Reno, Nevada, January 1988.

PERIDIER, V. J., WALKER, J. D. A. & SMITH, F. T. 1990 Vortex-induced boundary-layer separation. Parts I and II. *J. Fluid Mech.* (submitted). (1990); also presentations by Walker and Smith at Workshop on Unsteady Separation, Ohio State University, January 1990.

RIZZETTA, D. P., BURGGRAF, O. R. & JENSON, R. 1978 Triple-deck solutions for viscous supersonic and hypersonic flow past corners. *J. Fluid Mech.* **89**, 535–552.

RUBAN, A. I. 1978 *J. Vychisl. Mat. Fiz.* **18**, 1253–1265.

SMITH, F. T. 1977 The laminar separation of an incompressible fluid streaming past a smooth surface. *Proc. R. Soc. Lond.* A **356**, 433–463.

SMITH, F. T. 1982 On the high Reynolds number theory of laminar flows. *IMA J. Appl. Maths* **28**, 207–281.

SMITH, F. T. 1985 Two-dimensional disturbance travel, growth and spreading in boundary layers. *Utd Tech. Res. Center Rep.* 85–36.

SMITH, F. T. 1986*a* Two-dimensional disturbance travel, growth and spreading in boundary layers. *J. Fluid Mech.* **169**, 353–377.

SMITH, F. T. 1986*b* Steady and unsteady boundary-layer separation. *Ann. Rev. Fluid Mech.* **18**, 197–220.

SMITH, F. T. 1987 Separating flow: small-scale, large-scale, and nonlinear unsteady effects. In *Boundary-Layer Separation* (ed. S. N. Brown & F. T. Smith). Springer.

SMITH, F. T. 1988*a* A reversed-flow singularity in interacting boundary layers, (based on *Utd. Tech. Res. Cent. Rep* UT88-12) *Proc. R. Soc. Lond.* A **420**, 21–52.

SMITH, F. T. 1988*b* Finite-time break-up can occur in any unsteady interactive boundary-layer. *Mathematika* **35**, 256–273.

SMITH, F. T. & MERKIN, J. H. 1982 Triple-deck solutions for subsonic flow past humps, concave or convex corners and wedged trailing edges. *Computers Fluids* **10**, 7–25.

SMITH, F. T. & STEWARTSON, K. 1973 On slot-injection into a supersonic laminar boundary-layer. *Proc. R. Soc. Lond.* A **332**, 1–22.

STEWARTSON, K. 1974 Multi-structured boundary layers on flat plates and related bodies. *Adv. Appl. Mech.* **14**, 145–239.

STEWARTSON, K. 1981 D'Alembert's paradox. *SIAM REv.* **23**, 308–343.

STEWARTSON, K. & WILLIAMS, P. G. 1969 Self-induced separation. *Proc. R. Soc. Lond.* A **312**, 181–206.

STEWARTSON, K. & WILLIAMS, P. G. 1973 Self-induced separation II. *Mathematika* **20**, 98–108.

SYCHEV, V. V. 1987 *Asymptotic Theory of Separated Flows.* Moscow: Nauka.

VELDMAN, A. E. P. 1981 New quasi-simultaneous method to calculate interacting boundary layers. *AIAA J.* **19**, 79–85.

WERLE, M. J., BURGGRAF, O. R., RIZZETTA, D. P. & VATSA, V. N. 1979 *AIAA J.* **17**, 336–356.

WILLIAMS, B. R. 1989 Viscous–inviscid interaction schemes for separated flow. *Proc. R. Aero. Soc. Mtg, Prediction & Exploitation of Separated Flows, April 1989, London.*